Securing the Sustainability of Global Medical Nuclear Supply Chains Through Economic Cost Recovery, Risk Management, and Optimization

Anna Nagurney[1], Ladimer S. Nagurney[2], and Dong Li[1]

[1]Isenberg School of Management
University of Massachusetts, Amherst, Massachusetts 01003

[2]Department of Electrical and Computer Engineering
University of Hartford, West Hartford, CT 06117

Acknowledgments

This presentation is based on the paper:

Nagurney, A., Nagurney, L., and Li, D., 2012. Securing the Sustainability of Global Medical Nuclear Supply Chains Through Economic Cost Recovery, Risk Management, and Optimization,
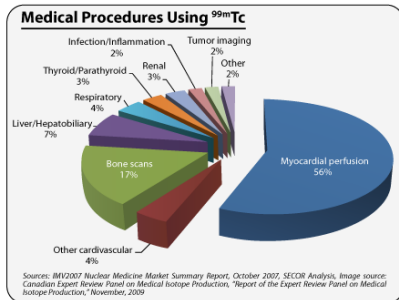
where a full list of references can be found.

- Background and Motivation

- The Sustainable Medical Nuclear Supply Chain Network Optimization Model

- The Computational Approach

- The Case Study

- Summary and Suggestions for Future Research

A radioactive isotope is bound to a pharmaceutical that is injected into the patient and travels to the site or organ of interest in order to construct an image for medical diagnostic purposes.

By using medical radioisotope techniques, health professionals can enable the earlier and more accurate detection of cardiac problems as well as cancer, the two most common causes of death (see Kochanek et al. (2011)).

Medical Procedures Using ^{99m}Tc

Infection/Inflammation 2%
Tumor imaging 2%
Thyroid/Parathyroid 3%
Renal 3%
Other 2%
Respiratory 4%
Liver/Hepatobiliary 7%
Bone scans 17%
Myocardial perfusion 56%
Other cardivascular 4%

Sources: IMV2007 Nuclear Medicine Market Summary Report, October 2007, SECOR Analysis, Image source: Canadian Expert Review Panel on Medical Isotope Production, "Report of the Expert Review Panel on Medical Isotope Production," November, 2009

Technetium, ^{99m}Tc, which is a decay product of Molybdenum-99, ^{99}Mo, is the most commonly used medical radioisotope, used in more than 80% of the radioisotope injections, with more than 30 million procedures worldwide each year.

Each day, 41,000 nuclear medical procedures are performed in the United States using Technetium-99m.

Over 100,000 hospitals in the world use radioisotopes (World Nuclear Association (2011)).

In 2008, 18.5 million doses of ^{99m}Tc were injected in the US with 2/3 of them used for cardiac exams, with the other uses including bone scans (Lantheur Medical Imaging, Inc (2009)).

For over two decades, all of the Molybdenum necessary for US-based nuclear medical diagnostic procedures, which include diagnostics for two of the greatest killers, cancer and cardiac problems, comes from foreign sources.

For over two decades, all of the Molybdenum necessary for US-based nuclear medical diagnostic procedures, which include diagnostics for two of the greatest killers, cancer and cardiac problems, comes from foreign sources.

Background and Motivation

All producing countries of ^{99}Mo, in principle, have agreed to convert to low enriched uranium (LEU).

Disadvantages:

LEU has a lower production yield than HEU and a greater number of targets needed to be irradiated with associated increased volumes of waste.

Indeed, according to Kramer (2011), the South African Nuclear Energy Corp (Necsa) believes that the LEU production process will approximately double the amount of waste generated in extracting the radioisotope, whereas other producers are likely to see a factor of four increase in their wastes.

[99]Mo Supply Chain Challenges:

- Limitations in processing capabilities make the world critically vulnerable to Molybdenum supply chain disruptions.

- Long-distance transportation of the product during raises safety and security risks, and also results in greater decay of the product. LEU targets can be transport by multiple modes including by air.

- The number of generator manufacturers is under a dozen (OECD Nuclear Energy Agency (2010b)).

- The majority of the reactors are between 40 and 50 years old. Several of the reactors currently used are due to be retired by the end of this decade(Seeverens (2010) and OECD Nuclear Energy Agency (2010a)).

Background and Motivation

We use a variational inequality formulation since such a formulation results in an elegant computational procedure.

- Nagurney, A., Aronson, J., 1989. A general dynamic spatial price network equilibrium model with gains and losses. Networks, 19, 751-769.

- Nagurney, A., Masoumi, A., Yu, M., 2012. Supply chain network operations management of a blood banking system with cost and risk minimization. Computational Management Science, 9(2), 205-231.

- Masoumi, A. H., Yu, M., and Nagurney, A., 2012. A supply chain generalized network oligopoly model for pharmaceuticals under brand differentiation and perishability. Transportation Research E, 48, 762-780.

Background and Motivation

Relevant papers that applied a generalized network approach in the modeling of optimization and equilibrium problems are as the following. Some of the theory in this presentation is from the first paper.

- Masoumi, A. H., Yu, M., and Nagurney, A., 2012. A supply chain generalized network oligopoly model for pharmaceuticals under brand differentiation and perishability. Transportation Research E, 48, 762-780.

- Nagurney, A., Masoumi, A., Yu, M., 2012. Supply chain network operations management of a blood banking system with cost and risk minimization. Computational Management Science, 9(2), 205-231.

- Yu, M., and Nagurney, A., 2012. Competitive food supply chain networks with application to fresh produce. European Journal of Operational Research, 223, 701-710.

In an earlier work,

Nagurney, A. and Nagurney, L., 2012. Medical nuclear supply chain design: A tractable network model and computational approach. International Journal of Production Economics, 140 (2), 865-874,

we focused on the design and redesign of medical nuclear supply chains, and the emphasis was on the long term.

Here, in contrast, our goal is to determine the true economic costs associated with this critical medical nuclear supply chain so as to optimize existing processes. We also focus on HEU versus LEU trade-offs in terms of waste and risk.

We model the supply chain network optimization problem as a multicriteria system-optimization problem.

- We identify the specific losses on the links/arcs through the use of the time decay of the radioisotope.

- We capture distinctions between LEU versus HEU target irradiation and processing.

- We consider total cost minimization associated with the operational costs, along with the waste management costs, and the associated risk of the various supply chain network activities since here the nuclear products are hazardous products and by-products.

The model's solution provides the optimal levels of production, transportation, and processing of the medical radioisotope.

We develop the economic cost recovery sustainable medical nuclear supply chain network optimization model, with a focus on ^{99}Mo, referred to, henceforth, as Mo. We note that the construction is also relevant, with minor modifications, to other radioisotopes, including Iodine-131.
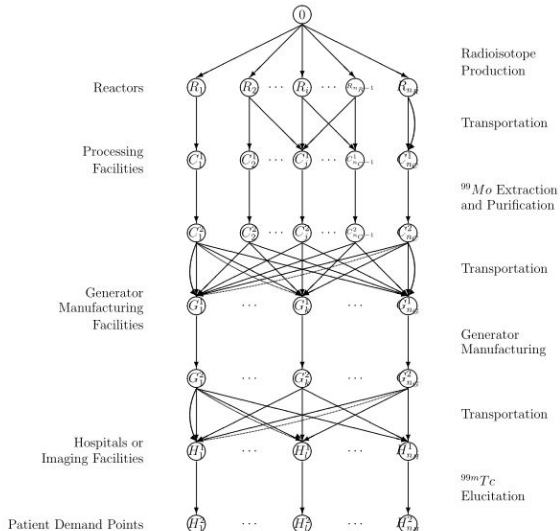
Figure: The Medical Nuclear Supply Chain Network Topology

$c_a(f_a)$: the unit operational cost function on link a.

f_a: the flow of the nuclear product on link a.

$\mathcal{P}_k$: the set of paths joining $(0, H_k^2)$.

$\mathcal{P}$: the set of all paths joining node 0 to the destination nodes.

$n_{\mathcal{P}}$: the number of paths.

x_p : the (initial) flow of Mo on path p.

d_k: the demand for the radioisotope at the demand point $H_k^2; k = 1, \ldots, n_H$.

α_a: the percentage of decay and additional loss over link a. It can be modeled as the product of the radioactive decay multiplier α_{d_a} and the processing loss multiplier α_{l_a}. $\alpha_a \in (0,1]$.

The Underlying Physics

The activity of a radioisotope (in disintegrations per unit time)

$$\frac{dN}{dt} \propto N, \tag{1}$$

where $N = N(t) =$ the quantity of a radioisotope.

The quantity of a radioisotope in a time interval t

$$N(t) = N_0 e^{-\lambda t}, \tag{2}$$

where N_0 is the quantity present at the beginning of the interval and λ is the decay constant of the radioisotope (see Berger, Goldsmith, and Lewis (2004)).

The Link and Path Multipliers

The half-life $t_{1/2}$

$$t_{1/2} = \frac{\ln 2}{\lambda}. \tag{3}$$

The value of $t_{1/2}$ for *Mo* is 66.7 hours.

The radioactive decay multiplier α_{d_a}

$$\alpha_{d_a} = e^{-\lambda t_a}, \tag{4}$$

$$\alpha_{d_a} = e^{-\lambda t_a} = e^{-\ln 2 \frac{t_a}{t_{1/2}}} = 2^{-\frac{t_a}{t_{1/2}}}. \tag{5}$$

where t_a is the time spent on link a.

Different processing links may have different values for the processing loss multiplier α_{l_a}:

- For transportation links, $\alpha_{l_a} = 1$.

- For the top-most manufacturing links, $\alpha_a = 1$.

The final flow on a link

$$f'_a = \alpha_a f_a, \qquad \forall a \in L. \tag{6}$$

Total discarding cost function on link a

$$\hat{z}_a = \hat{z}_a(f_a), \qquad \forall a \in L. \tag{7}$$

total operational cost on link a

$$\hat{c}_a(f_a) = f_a \times c_a(f_a), \qquad \forall a \in L. \tag{8}$$

The total operation cost functions and the total discarding functions are assumed to be convex and continuously differentiable.

Nonnegative link

$$x_p \geq 0, \qquad \forall p \in \mathcal{P}, \tag{9}$$

Path multiplier

$$\mu_p \equiv \prod_{a \in p} \alpha_a, \qquad \forall p \in \mathcal{P}, \tag{10}$$

where μ_p denote the multiplier corresponding to the loss on path p. Thus the projected demand at demand point R_k is

Projected demand

$$d_k \equiv \sum_{p \in \mathcal{P}_k} \mu_p x_p, \qquad k = 1, \ldots, n_H. \tag{11}$$

Relationship between link flows and path flows

$$
\alpha_{ap} \equiv \left\{
\begin{array}{ll}
\delta_{ap} \displaystyle\prod_{a' < a} \alpha_{a'}, & \text{if } \{a' < a\} \neq \emptyset, \\
\\
\delta_{ap}, & \text{if } \{a' < a\} = \emptyset,
\end{array}
\right.
\tag{12}
$$

where $\{a' < a\}$ denotes the set of the links preceding link a in path p, and δ_{ap} is defined as equal to one if link a is contained in path p; otherwise, it is equal to zero, therefore

$$
f_a = \sum_{p \in \mathcal{P}} x_p \, \alpha_{ap}, \qquad \forall a \in L.
\tag{13}
$$

The total cost minimization objective

$$\text{Minimize} \quad \sum_{a \in L} \hat{c}_a(f_a) + \sum_{a \in L} \hat{z}_a(f_a) \tag{14}$$

subject to: constraints (9), (11), and (13), and

$$f_a \leq \bar{u}_a, \qquad \forall a \in L. \tag{15}$$

The total risk function on link a

$$\hat{r}_a = \hat{r}_a(f_a), \quad \forall a \in L. \tag{16}$$

The total risk functions are assumed to be convex and continuously differentiable.

For a transportation link a, the total risk function would measure the impact of the travel time, the population density that the transportation route goes through, the unit probability of an accident using the particular mode represented by the link, the area of the impact zone, the length of the link, etc., and, ideally, also include impact of human factors.

In the case of a non-transportation processing link, the function would capture analogous aspects but with a focus on the specific processing activity.

The minimization of total costs is not the only objective. A major challenge for a medical nuclear organization is to capture the risk associated with different activities in the nuclear supply chain network.

The Risk Minimization Objective Function

$$\text{Minimize} \quad \sum_{a \in L} \hat{r}_a(f_a). \tag{17}$$

The multicriteria optimization problem in terms of link flow

$$\text{Minimize} \quad \sum_{a \in L} \hat{c}_a(f_a) + \sum_{a \in L} \hat{z}_a(f_a) + \omega \sum_{a \in L} \hat{r}_a(f_a) \quad (18)$$

subject to: constraints: (9), (11), (13), and (15).

The multicriteria optimization problem in terms of path flow

$$\text{Minimize} \quad \sum_{p \in \mathcal{P}} (\hat{C}_p(x) + \hat{Z}_p(x)) + \omega \sum_{p \in \mathcal{P}} \hat{R}_p(x) \qquad (19)$$

subject to: constraints (9), (11), and (15),

The total cost on path p:

$$\hat{C}_p(x) = x_p \times C_p(x), \forall p \in \mathcal{P}, \quad (20a)$$

$$\hat{Z}_p(x) = x_p \times Z_p(x), \forall p \in \mathcal{P}, \quad (20b)$$

$$\hat{R}_p(x) = x_p \times R_p(x), \forall p \in \mathcal{P}, \quad (20c)$$

The unit cost functions on path p, in turn, defined as:

$$C_p(x) \equiv \sum_{a \in L} c_a(f_a)\alpha_{ap}, \forall p \in \mathcal{P}, \quad (21a)$$

$$Z_p(x) \equiv \sum_{a \in L} z_a(f_a)\alpha_{ap}, \forall p \in \mathcal{P}, \quad (21b)$$

$$R_p(x) \equiv \sum_{a \in L} r_a(f_a)\alpha_{ap}, \forall p \in \mathcal{P}, \quad (21c)$$

We associate the Lagrange multiplier γ_a with constraint (15) for each link a, and we denote the optimal Lagrange multiplier by $\gamma_a^*, \forall a \in L$. The Lagrange multipliers may be interpreted as shadow prices. We group these Lagrange multipliers into the vector γ.

Let K denote the feasible set such that:

$$K \equiv \{(x, \gamma)|x \in R_+^{n_p}, (11) \text{ and } (15) \text{ hold}, \gamma \in R_+^{n_L}\}. \qquad (22)$$

We assume that the feasible set is nonempty.

Theorem

The optimization problem (19), subject to its constraints, is equivalent to the variational inequality problem: determine the vector of optimal path flows and the vector of optimal Lagrange multipliers $(x^*, \gamma^*) \in K$, such that:

$$\sum_{k=1}^{n_R} \sum_{p \in \mathcal{P}_k} \left[\frac{\partial(\sum_{q \in \mathcal{P}} \hat{C}_q(x^*))}{\partial x_p} + \frac{\partial(\sum_{q \in \mathcal{P}} \hat{Z}_q(x^*))}{\partial x_p} \right.$$

$$\left. + \sum_{a \in L} \gamma_a^* \delta_{ap} + \omega \frac{\partial(\sum_{q \in \mathcal{P}} \hat{R}_q(x^*))}{\partial x_p} \right] \times [x_p - x_p^*]$$

$$+ \sum_{a \in L} \left[\bar{u}_a - \sum_{p \in \mathcal{P}} x_p^* \alpha_{ap} \right] \times [\gamma_a - \gamma_a^*] \geq 0, \quad \forall(x, \gamma) \in K. \quad (24)$$

Theorem

determine the vector of optimal link flows and the vector of optimal Lagrange multipliers $(f^*, \gamma^*) \in K^1$, such that:

$$\sum_{a \in L} \left[\frac{\partial \hat{c}_a(f_a^*)}{\partial f_a} + \frac{\partial \hat{z}_a(f_a^*)}{\partial f_a} + \gamma_a^* + \omega \frac{\partial \hat{r}_a(f_a^*)}{\partial f_a} \right] \times [f_a - f_a^*]$$

$$+ \sum_{a \in L} [\bar{u}_a - f_a^*] \times [\gamma_a - \gamma_a^*] \geq 0, \qquad \forall (f, \gamma) \in K^1, \qquad (25)$$

where K^1 denotes the feasible set:

$$K^1 \equiv \{(f, \gamma) | \exists x \geq 0, \ (9), (11), (13), and (15) \text{ hold, and } \gamma \geq 0\}.$$
$$(26)$$

We propose the modified projection method (Korpelevich (1977)) in path flows. This algorithm, in the context of our new model, yields subproblems that can be solved exactly, and in closed form, for the path flows, using a variant of the exact equilibration algorithm, adapted to incorporate arc/path multipliers, along with explicit formulae for the Lagrange multipliers.

The modified projection is guaranteed to converge if the function F that enters the variational inequality satisfies monotonicity and Lipschitz continuity (see Nagurney (1999)) and that a solution exists, which is the case for our model.

The Computational Approach

$\mathcal{T}$ denotes an iteration counter.

The modified projection method

Step 0: Initialization
Set $X^0 \in \mathcal{K}$. Let $\mathcal{T} = 1$ and let η be a scalar such that $0 < \eta \leq \frac{1}{L}$, where L is the Lipschitz continuity constant.

Step 1: Computation
Compute $\tilde{X}^{\mathcal{T}}$ by solving the VI subproblem:

$$\langle \tilde{X}^{\mathcal{T}} + \eta F(X^{\mathcal{T}-1}) - X^{\mathcal{T}-1}, X - \tilde{X}^{\mathcal{T}} \rangle \geq 0, \quad \forall X \in \mathcal{K}. \quad (29)$$

Step 2: Adaptation
Compute $X^{\mathcal{T}}$ by solving the VI subproblem:

$$\langle X^{\mathcal{T}} + \eta F(\tilde{X}^{\mathcal{T}}) - X^{\mathcal{T}-1}, X - X^{\mathcal{T}} \rangle \geq 0, \quad \forall X \in \mathcal{K}. \quad (30)$$

Step 3: Convergence Verification
If $\max |X_l^{\mathcal{T}} - X_l^{\mathcal{T}-1}| \leq \epsilon$, for all l, with $\epsilon > 0$, a prespecified tolerance, then stop; else, set $\mathcal{T} =: \mathcal{T} + 1$, and go to Step 1.

Explicit Formulae for the Lagrange Multipliers at Step 1 (cf. (29))

$$\tilde{\gamma}_a^{\mathcal{T}} = \max\{0, \gamma_a^{\mathcal{T}-1} + \eta(\sum_{p \in \mathcal{P}} x_p^{\mathcal{T}-1}\delta_{ap} - \bar{u}_a)\}, \quad \forall a \in L. \qquad (31)$$

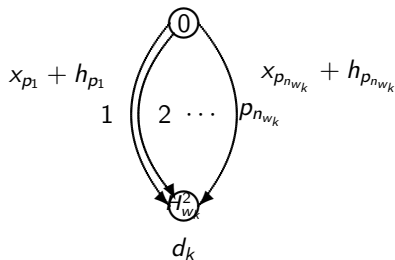The induced path flow subproblems in (29) and (30) have a special network structure of the form given in Figure 2.

Figure: Special Network Structure of an Induced Path Flow Subproblem for Each Demand Point k

The Computational Approach

The path flow subproblems that one must solve in Step 1 (see (29)) have the following form for each demand point k; $k = 1, \ldots, n_H$:

$$\text{Minimize} \quad \frac{1}{2} \sum_{p \in \mathcal{P}_k} x_p^2 + \sum_{p \in \mathcal{P}_k} h_p x_p \tag{32}$$

subject to:

$$d_k \equiv \sum_{p \in \mathcal{P}_k} \mu_p x_p, \tag{33}$$

$$x_p \geq 0, \quad \forall p \in \mathcal{P}_k, \tag{34}$$

where

$$h_p \equiv x_p^{\mathcal{T}-1} - \eta \left[\frac{\partial(\sum_{q \in \mathcal{P}} \hat{C}_q(x^{\mathcal{T}-1}))}{\partial x_p} + \frac{\partial(\sum_{q \in \mathcal{P}} \hat{Z}_q(x^{\mathcal{T}-1}))}{\partial x_p} + \right.$$

$$\left. \sum_{a \in L} \gamma_a^{\mathcal{T}-1} \delta_{ap} + \omega \frac{\partial(\sum_{q \in \mathcal{P}} \hat{R}_q(x^{\mathcal{T}-1}))}{\partial x_p} \right]$$

.

The Computational Approach

An Exact Equilibration Algorithm for a Generalized Specially Structured Network

Step 0: Sort

Sort the fixed terms $\frac{h_p}{\mu_p}$; $p \in \mathcal{P}_k$ in nondescending order and relabel the paths/links accordingly. Assume, from this point on, that they are relabeled. Set $r = 1$.

Step 1: Computation

Compute

$$\lambda_{w_k}^r = \frac{\sum_{i=1}^{r} \mu_{p_i} h_{p_i} + d_k}{\sum_{i=1}^{r} \mu_{p_i}^2}. \tag{35}$$

Step 2: Evaluation

If $\frac{h_{p_r}}{\mu_{p_r}} < \lambda_k^r \leq \frac{h_{p_{r+1}}}{\mu_{p_{r+1}}}$, then stop; set $s = r$ and go to Step 3; otherwise, let $r = r + 1$ and return to Step 1. If $r = n_k$, where n_k denotes the number of paths connecting destination node H_k^2 with origin node 0, then set $s = n_k$ and go to Step 3.

Step 3: Path Flow Determination

Set

$$x_{p_i} = \mu_p \lambda_k^s - h_{p_i}, \quad i = 1, \ldots, s.$$
$$x_{p_i} = 0, \quad i = s + 1, \ldots, n_k. \tag{36}$$

The modified projection method is guaranteed to converge to a solution of the medical nuclear supply chain network problem provided that the function F (cf. (28)) is monotone and Lipschitz continuous. Monotonicity follows under our imposed assumptions and Lipschitz continuity will also hold provided that the marginal total cost and marginal risk functions have bounded second order partial derivatives.

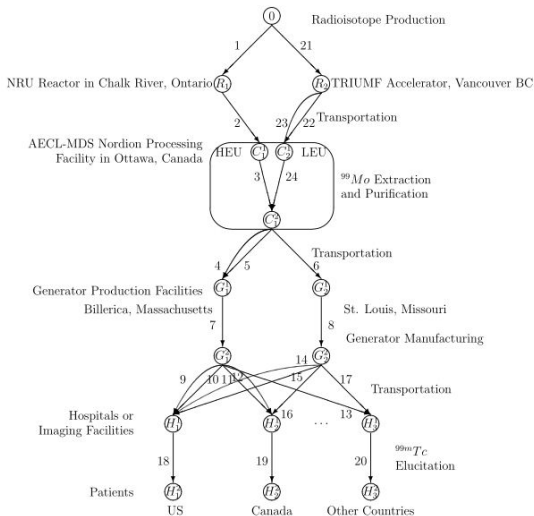Figure: The Medical Nuclear Supply Chain Topology for ^{99}Mo from Canada to the United States, Canada, and Other Countries

The transportation links are assumed not to be capacity limited (that is, we assume very large capacities). In the computations, we set the value to 5,000,000 for all such links.

We implemented the modified projection method, along with the generalized exact equilibration algorithm, for the solution of our medical nuclear supply chain network case study. The ϵ in the convergence criterion was 10^{-6}.

We calculated the values of the arc multipliers α_{da}, for all links $a = 1, \ldots, 24$, using data in the OECD (2010a) report and in the National Research Council (2009) report.

Operating cost data were taken from OECD (2010b) and converted to per Curie processed or generated.

The functional form of $\hat{z}_a(f_a)$ should be consistent with $\hat{c}_a(f_a)$. Moreover, the discarding cost of LEU processing (link 24) should be about twice the discarding costs for the HEU processing (link 3), the costs of discarding during elucitation are higher in the US (link 18) as compared to other countries (links 19 and 20).

The risk functions for transportation links were estimated based upon the overall accident rate per kilometer for aircraft and trucks carrying nuclear material as reported in Resnikoff (1992).

We assumed three demand points corresponding, respectively, to the collective demands in the US, in Canada, and in other countries.

The demands were : $d_1 = 3,600$, $d_2 = 1,800$, and $d_3 = 1,000$ and these denote the demands, in Curies, per week. These values were obtained by using the daily number of procedures in the US and extrapolating for the others.

The Case Study-Example 1

The weight ω was set equal to 1 in Example 1.

Link a	α_a	$\hat{c}_a(f_a)$	$\hat{z}_a(f_a)$	$\hat{r}_a(f_a)$	$\bar{u}_a$	f_a^*	λ_a^*
1	1.00	$2f_1^2 + 25.6f_1$	0.00	$2.00 \times 10^{-2}f_1$	33,353	9720.20	0.00
2	.969	$f_2^2 + 5f_2$	0.00	$3.18 \times 10^{-1}f_2$	large	9720.20	0.00
3	.706	$5f_3^2 + 192f_3$	$5f_3^2 + 80f_3$	$2.00 \times 10^{-3}f_3$	32,154	9419.35	0.00
4	.920	$2f_4^2 + 4f_4$	0.00	$1.59 \times 10^{-1}f_4$	large	3045.90	0.00
5	.901	$f_5^2 + f_5$	0.00	$2.16 \times 10^{-3}f_5$	large	2327.34	0.00
6	.915	$f_6^2 + 2f_6$	0.00	$6.9 \times 10^{-3}f_6$	large	4934.45	0.00
7	.804	$f_7^2 + 166f_7$	$2f_7^2 + 7f_7$	$2.00 \times 10^{-4}f_7$	19,981	4899.16	0.00
8	.804	$f_8^2 + 166f_8$	$2f_7^2 + 7f_7$	$2.00 \times 10^{-4}f_8$	19,981	4515.02	0.00
9	.883	$2f_9^2 + 4f_9$	0.00	$2.00 \times 10^{-4}f_9$	large	1623.06	0.00
10	.779	$f_{10}^2 + 1f_{10}$	0.00	$1.47 \times 10^{-2}f_{10}$	large	0.00	0.00
11	.883	$2f_{11}^2 + 4f_{11}$	0.00	$2.00 \times 10^{-4}f_{11}$	large	2038.51	0.00
12	.688	$f_{12}^2 + 2f_{12}$	0.00	$1.47 \times 10^{-2}f_{12}$	large	0.00	0.00
13	.688	$2.5f_{13}^2 + 2f_{13}$	0.00	$1.98 \times 10^{-4}f_{13}$	large	277.36	0.00
14	.883	$2f_{14}^2 + 2f_{14}$	0.00	$7.33 \times 10^{-3}f_{14}$	large	2453.95	0.00
15	.779	$f_{15}^2 + 7f_{15}$	0.00	$1.00 \times 10^{-4}f_{15}$	large	0.00	0.00
16	.688	$2f_{16}^2 + 4f_{16}$	0.00	$1.00 \times 10^{-4}f_{16}$	large	0.00	0.00
17	.688	$2f_{17}^2 + 6f_{17}$	0.00	$1.98 \times 10^{-5}f_{17}$	large	1176.13	0.00
18	1.00	$2f_{18}^2 + 800f_{18}$	$4f_{18}^2 + 80f_{18}$	$2.00 \times 10^{-5}f_{18}$	5,000	3600.00	0.00
19	1.00	$f_{19}^2 + 600f_{19}$	$1f_{19}^2 + 60f_{19}$	$2.00 \times 10^{-5}f_{19}$	3,000	1800.00	0.00
20	1.00	$f_{20}^2 + 300f_{20}$	$1f_{20}^2 + 30f_{20}$	$2.00 \times 10^{-5}f_{20}$	2,000	1000.00	0.00
21	1.00	$4f_{21}^2 + 50f_{21}$	0.00	$2.00 \times 10^{-2}f_{21}$	10,006	5867.24	0.00
22	.436	$6f_{22}^2 + 6f_{22}$	0.00	$1.04 \times 10^1 f_{22}$	large	0.00	0.00
23	.883	$3f_{23}^2 + 21f_{23}$	0.00	$1.44 \times 10^{-2}f_{23}$	large	5867.24	0.00
24	.706	$5f_{24}^2 + 192f_{24}$	$10f_{24}^2 + 160f_{24}$	$2.00 \times 10^{-3}f_{24}$	10,006	5180.77	0.00

Highlights of Example 1

- None of the links were operated at full capacity.

- The transportation links 10, 12, 15, 16, and 22 have zero flow.

- As speculated by Kramer (2011), that the new LEU production facility (cf. link 21) is expected to produce about 30% of the needs, and this was also the result obtained in our computation.

- The value of the objective function (cf. (18)) was: 2,096,149,888.00 whereas the total risk (cf. (17)) was: 4,060.81.

- The demand was met at the demand points but, given the perishability of the radioisotope, many more Curies had to be produced and processed.

Case Study-Example 2

Example 2 is with a weight ω of 1000. The remainder of the input data were as in Table 1.

Link a	α_a	$\hat{c}_a(f_a)$	$\hat{z}_a(f_a)$	$\hat{r}_a(f_a)$	$\bar{u}_a$	f_a^*	λ_a^*
1	1.00	$2f_1^2 + 25.6f_1$	0.00	$2.00 \times 10^{-2} f_1$	33,353	9716.86	0.00
2	.969	$f_2^2 + 5f_2$	0.00	$3.18 \times 10^{-1} f_2$	large	9716.86	0.00
3	.706	$5f_3^2 + 192f_3$	$5f_3^2 + 80f_3$	$2.00 \times 10^{-3} f_3$	32,154	9415.64	0.00
4	.920	$2f_4^2 + 4f_4$	0.00	$1.59 \times 10^{-1} f_4$	large	3020.34	0.00
5	.901	$f_5^2 + f_5$	0.00	$2.16 \times 10^{-3} f_5$	large	2350.27	0.00
6	.915	$f_6^2 + 2f_6$	0.00	$6.9 \times 10^{-3} f_6$	large	4937.57	0.00
7	.804	$f_7^2 + 166f_7$	$2f_7^2 + 7f_7$	$2.00 \times 10^{-4} f_7$	19,981	4896.31	0.00
8	.804	$f_8^2 + 166f_8$	$2f_7^2 + 7f_7$	$2.00 \times 10^{-4} f_8$	19,981	4517.88	0.00
9	.883	$2f_9^2 + 4f_9$	0.00	$2.00 \times 10^{-4} f_9$	large	1622.27	0.00
10	.779	$f_{10}^2 + 1f_{10}$	0.00	$1.47 \times 10^{-2} f_{10}$	large	0.00	0.00
11	.883	$2f_{11}^2 + 4f_{11}$	0.00	$2.00 \times 10^{-4} f_{11}$	large	2038.51	0.00
12	.688	$f_{12}^2 + 2f_{12}$	0.00	$1.47 \times 10^{-2} f_{12}$	large	0.00	0.00
13	.688	$2.5f_{13}^2 + 2f_{13}$	0.00	$1.98 \times 10^{-4} f_{13}$	large	275.86	0.00
14	.883	$2f_{14}^2 + 2f_{14}$	0.00	$7.33 \times 10^{-3} f_{14}$	large	2454.74	0.00
15	.779	$f_{15}^2 + 7f_{15}$	0.00	$1.00 \times 10^{-4} f_{15}$	large	0.00	0.00
16	.688	$2f_{16}^2 + 4f_{16}$	0.00	$1.00 \times 10^{-4} f_{16}$	large	0.00	0.00
17	.688	$2f_{17}^2 + 6f_{17}$	0.00	$1.98 \times 10^{-5} f_{17}$	large	1177.63	0.00
18	1.00	$2f_{18}^2 + 800f_{18}$	$4f_{18}^2 + 80f_{18}$	$2.00 \times 10^{-5} f_{18}$	5,000	3600.00	0.00
19	1.00	$f_{19}^2 + 600f_{19}$	$1f_{19}^2 + 60f_{19}$	$2.00 \times 10^{-5} f_{19}$	3,000	1800.00	0.00
20	1.00	$f_{20}^2 + 300f_{20}$	$1f_{20}^2 + 30f_{20}$	$2.00 \times 10^{-5} f_{20}$	2,000	1000.00	0.00
21	1.00	$4f_{21}^2 + 50f_{21}$	0.00	$2.00 \times 10^{-2} f_{21}$	10,006	5872.24	0.00
22	.436	$6f_{22}^2 + 6f_{22}$	0.00	$1.04 \times 10^1 f_{22}$	large	0.00	0.00
23	.883	$3f_{23}^2 + 21f_{23}$	0.00	$1.44 \times 10^{-2} f_{23}$	large	5872.24	0.00
24	.706	$5f_{24}^2 + 192f_{24}$	$10f_{24}^2 + 160f_{24}$	$2.00 \times 10^{-3} f_{24}$	10,006	5185.19	0.00

- The same links as in Example 1 had zero flows.

- The value of the objective function was now: 2,100,204,416.00 and the total risk was now: 4,055.70.

- Note, for example, that the link flows shifted from links with higher total risk to those with lower total risk, such as the shift from link 1 to link 21.

Case Study-Example 3

We considered a medical nuclear supply chain disruption in the form of the NRU reactor's capacity being reduced to 9000.

Link a	α_a	$\hat{c}_a(f_a)$	$\hat{z}_a(f_a)$	$\hat{r}_a(f_a)$	$\bar{u}_a$	f_a^*	λ_a^*
1	1.00	$2f_1^2 + 25.6f_1$	0.00	$2.00 \times 10^{-2}f_1$	9000.00	9000.00	49667.88
2	.969	$f_2^2 + 5f_2$	0.00	$3.18 \times 10^{-1}f_2$	large	9000.00	0.00
3	.706	$5f_3^2 + 192f_3$	$5f_3^2 + 80f_3$	$2.00 \times 10^{-3}f_3$	32,154	8722.89	0.00
4	.920	$2f_4^2 + 4f_4$	0.00	$1.59 \times 10^{-1}f_4$	large	3173.72	0.00
5	.901	$f_5^2 + f_5$	0.00	$2.16 \times 10^{-3}f_5$	large	2168.41	0.00
6	.915	$f_6^2 + 2f_6$	0.00	$6.9 \times 10^{-3}f_6$	large	4962.43	0.00
7	.804	$f_7^2 + 166f_7$	$2f_7^2 + 7f_7$	$2.00 \times 10^{-4}f_7$	19,981	4873.56	0.00
8	.804	$f_8^2 + 166f_8$	$2f_7^2 + 7f_7$	$2.00 \times 10^{-4}f_8$	19,981	4540.62	0.00
9	.883	$2f_9^2 + 4f_9$	0.00	$2.00 \times 10^{-4}f_9$	large	1612.58	0.00
10	.779	$f_{10}^2 + 1f_{10}$	0.00	$1.47 \times 10^{-2}f_{10}$	large	0.00	0.00
11	.883	$2f_{11}^2 + 4f_{11}$	0.00	$2.00 \times 10^{-4}f_{11}$	large	2038.51	0.00
12	.688	$f_{12}^2 + 2f_{12}$	0.00	$1.47 \times 10^{-2}f_{12}$	large	0.00	0.00
13	.688	$2.5f_{13}^2 + 2f_{13}$	0.00	$1.98 \times 10^{-4}f_{13}$	large	267.26	0.00
14	.883	$2f_{14}^2 + 2f_{14}$	0.00	$7.33 \times 10^{-3}f_{14}$	large	2464.43	0.00
15	.779	$f_{15}^2 + 7f_{15}$	0.00	$1.00 \times 10^{-4}f_{15}$	large	0.00	0.00
16	.688	$2f_{16}^2 + 4f_{16}$	0.00	$1.00 \times 10^{-4}f_{16}$	large	0.00	0.00
17	.688	$2f_{17}^2 + 6f_{17}$	0.00	$1.98 \times 10^{-5}f_{17}$	large	1186.23	0.00
18	1.00	$2f_{18}^2 + 800f_{18}$	$4f_{18}^2 + 80f_{18}$	$2.00 \times 10^{-5}f_{18}$	5,000	3600.00	0.00
19	1.00	$f_{19}^2 + 600f_{19}$	$1f_{19}^2 + 60f_{19}$	$2.00 \times 10^{-5}f_{19}$	3,000	1800.00	0.00
20	1.00	$f_{20}^2 + 300f_{20}$	$1f_{20}^2 + 30f_{20}$	$2.00 \times 10^{-5}f_{20}$	2,000	1000.00	0.00
21	1.00	$4f_{21}^2 + 50f_{21}$	0.00	$2.00 \times 10^{-2}f_{21}$	10,006	6650.96	0.00
22	.436	$6f_{22}^2 + 6f_{22}$	0.00	$1.04 \times 10^1 f_{22}$	large	0.00	0.00
23	.883	$3f_{23}^2 + 21f_{23}$	0.00	$1.44 \times 10^{-2}f_{23}$	large	6650.96	0.00
24	.706	$5f_{24}^2 + 192f_{24}$	$10f_{24}^2 + 160f_{24}$	$2.00 \times 10^{-3}f_{24}$	10,006	5872.80	0.00

- The value of the objective function was now: 2,117,958,400.00 and the total risk was: 3865.07. Interestingly, this was the lowest value obtained in the three examples.

- For this example, the total risk decreased even more significantly than that observed in Example 2 relative to Example 1.

- As the capacity associated with link 1 decreased, the link flows shifted to links with higher capacities and larger arc multipliers, such as the shift from link 1 to 21, and the shift from link 5 to link 4.

We developed a new model of sustainable medical nuclear supply chain operations management that incorporates:

- the time-dependent and perishable nature of radioisotopes, and

- the hazardous aspects which affect not only the transportation modes but also waste management and risk management issues.

The model is a generalized network model that includes multicriteria decision-making so that

- the organization can minimize total operating and

- the waste management costs, as well as

- the risk associated with the various medical nuclear supply chain network activities of processing, generator production, transportation, and ultimate usage in medical procedures at hospitals and other appropriate medical facilities.

Our model also traces the amount of the radioisotope that is left as a particular pathway of the supply chain is traversed.

Summary and Suggestions for Future Research

- The formulation of the model and the qualitative analysis exploit the theory of variational inequalities since it yields a very elegant procedure for computational purposes.

- Moreover, it provides us with the foundation to explore other scenarios as the technology landscape continues to evolve and to bring other participants into medical nuclear production.

- A numerical case study based on North America, with the focus of an existing HEU reactor and an LEU accelerator that is expected to come online soon, reveals the generality and practicality of our framework.

An interesting question for future research would be the investigation of various types of possible competition associated with, for example, transportation service providers in the medical nuclear supply chain arena as well as competition among the generator manufacturing facilities.

To develop such models one may utilize some of the concepts associated with competitive multitiered supply chain network equilibrium problems governed by Nash equilibria (see, e.g., Nagurney (2006)).

In addition it would be interesting to construct a bi-objective version of this model and analyze the Pareto set of solutions.

For more information, please visit http://supernet.isenberg.umass.edu.